



Intrinsic aberration coefficients for plane-symmetric optical systems consisting of spherical surfaces

YUXUAN LIU,  JESSICA STEIDLE,  AND JANNICK P. ROLLAND* 

The Institute of Optics, University of Rochester, 275 Hutchison Rd, Rochester, New York 14627, USA

*Corresponding author: rolland@optics.rochester.edu

Received 13 October 2022; revised 21 December 2022; accepted 22 December 2022; posted 22 December 2022; published 20 January 2023

This paper presents the analytical form of the intrinsic aberration coefficients for spherical plane-symmetric optical systems expressed as a function of first-order system parameters and the paraxial chief and marginal ray angles and heights. The derived aberration coefficients are in the third and fourth groups with the multiplication of two or three vector products of pupil and field vectors. © 2023 Optica Publishing Group under the terms of the [Optica Open Access Publishing Agreement](#)

<https://doi.org/10.1364/JOSAA.477962>

1. INTRODUCTION

While lens design has historically focused on optical systems that have rotational symmetry about the optical axis, there have been increasing efforts to study and design non-rotationally symmetric systems, including freeform optics [1]. By using a system off-axis in the field or aperture, the rotational symmetry can be broken to achieve unobscured reflective systems. Offner designed a unit magnification relay using field bias [2]. Cook used an offset field and an offset aperture to form the unobscured three-mirror anastigmat [3]. The rotational symmetry can also be broken by tilting or decentering optical surfaces. Small tilts and decenters often occur in the manufacturing and assembly process chain, which was investigated independently by both Conrady [4] and Epstein [5]. Cook used perturbative tilts and decenters to improve performance in the final optimization stage [6]. Another way of breaking symmetry is to use rotationally non-symmetric surface types. Early research was done on anamorphic surfaces independently by both Wynne [7] and Sands [8].

In the studies mentioned above, the symmetry was broken by deviating from a parent rotationally symmetric system. Alternatively, Buchroeder introduced tilted-component optical systems as a new class of rotationally non-symmetric systems that do not evolve from any parent systems [9]. Buchroeder described these systems using a principal ray passing through the vertex of each surface. This description method maintains the properties of Gaussian optics and is a natural generalization of the on-axis sequential description method. With the recent emergence of freeform optics [1], more systems are designed without dependence on rotationally symmetric starting points [10–12].

There has been a strong interest in formulating new aberration theories and design methods for systems that do not depend on rotationally symmetric parent systems. Buchroeder found that the aberration contribution from a spherical surface is symmetric about the local axis that connects the center of curvature and the center of the pupil [9]. Shack and Thompson expanded the wave aberration theory of Hopkins [13] in the development of nodal aberration theory (NAT) [14–18] to express the effect of tilt and decenter on the aberration field. Fuerschbach *et al.* used NAT to derive the formulae for the wave aberrations caused by Zernike freeform surfaces [19]. Bauer *et al.* utilized these formulae in a design method based on analyzing the potential of folding geometries to correct aberrations [20]. Aberration theories based on ray tracing were also proposed. Tang and Gross utilized a mixed ray-tracing method to calculate surface aberration contribution and differentiate intrinsic and induced (extrinsic) aberration components in symmetry-free optical systems [21,22]. This method does not express aberrations as functions of system parameters, and therefore cannot provide information on how system parameters affect the aberrations. Caron and Bäumer developed a matrix formalism based on a set of generalized ray-tracing equations [23,24] to derive ray aberration coefficients for reflective optical systems and gave an illustration of ray aberration coefficients for N-mirror confocal systems where recursive relations between N-mirror and N + 1-mirror systems were used [25]. An important question is whether the recursive relations are valid for more general non-confocal systems, since the derivation through matrix multiplication becomes increasingly complex as the number of mirrors increases.

In a different approach to rotationally asymmetric systems, specifically systems with bilateral symmetry, Sasian built on

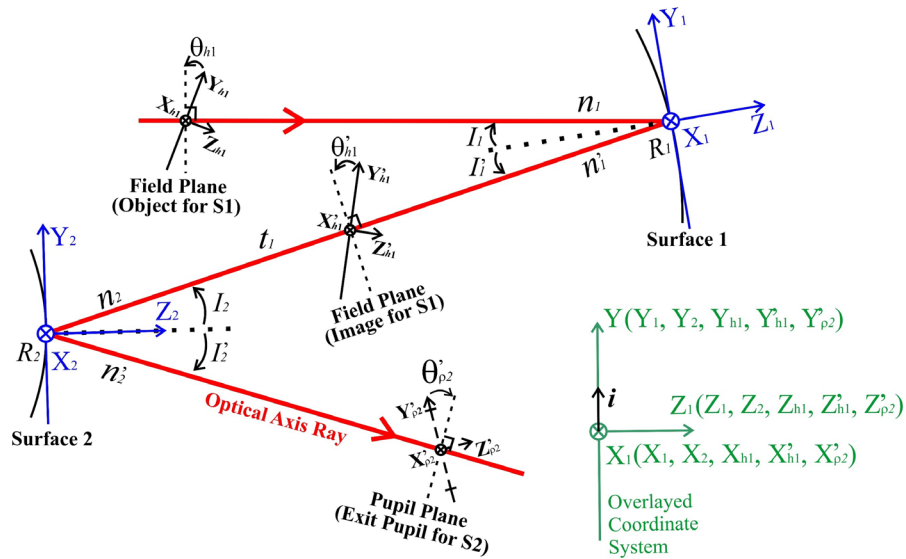


Fig. 1. Illustration of the system description in the plane of symmetry (not a real system). In green the overlaid coordinate system where all local coordinate systems for surfaces, field, and pupil planes coincide, with i being the common unit vector in the Y direction.

the vectorial expression of wavefront aberrations and grouped various aberrations based on the number of vector products in the aberration expression. He derived the aberration coefficients in the third group for plane-symmetric (bilateral-symmetric) systems, which are expressed in system parameters such as the radius of curvature, the distance between surface vertices, and the tilt angle [26]. The expressions help analyze surface contributions and the impact of parameters. This paper expands the aberration coefficients to the fourth group for plane-symmetric systems. This expansion enables the ability to analytically describe higher-order aberrations in plane-symmetric systems, raising the accuracy of the aberration theory in predicting the image quality of plane-symmetric systems. This expansion to the fourth group is especially important for systems with a large field and a fast F -number where higher-order aberrations are significant. Section 2 reviews and illustrates the description method for plane-symmetric systems. Section 3 reviews the paraxial optics used in the derivation process. In Section 4, the fourth group's coefficients are defined as pupil and field dependence functions. In Section 5, an overview of the derivation process is provided. Section 6 lists the formulae for the aberration coefficients in the fourth group from the derivations performed. Section 7 provides an example that compares aberration coefficients calculated from the formulae and from ray tracing in CODE V lens design software.

2. PLANE-SYMMETRIC SYSTEM DESCRIPTION

The analytical form of the aberration coefficients is determined by which system parameters are used to describe the optical system. This paper follows the system parametrization method by Sasian [26] that describes a system following an optical axis ray (OAR) connecting the center of the object and the center of the aperture stop of the system. This OAR lies in the plane of symmetry, as shown in Fig. 1, intersecting each optical surface where the vertex of the surface is defined. The system is described sequentially with the location of each surface depending on that of the previous surface by two parameters: the distance between

the vertices, t , and the incident angle of the OAR at the vertex, I . The field and pupil planes are defined with their centers along the OAR and with tilt angles, θ_b for field planes and θ_p for pupil planes, as shown in Fig. 1. All parameters and local coordinate systems can have a numerical subscript denoting the surface they correspond to. In addition, a prime symbol indicates that the parameter is in the image space of the surface. The refractive index, n , and the field and pupil plane tilt angles defined in the image space of one surface are equal to that defined in the object space of the next surface.

A local right-handed Cartesian coordinate system is set up for each surface as well as each field or pupil plane with its origin at the point where the OAR intersects the surface, the Z axis of the local coordinate systems along the surface normal, and the YZ plane in the plane of symmetry. The positive Z direction of each local coordinate system points toward the propagation direction of the OAR before the surface if the OAR has undergone an even number of reflections preceding the surface; otherwise, the positive Z direction points in the opposite direction. This parameterization method can be applied to both reflective and refractive systems. An example of a reflective case is shown in Fig. 1.

All parameters in Fig. 1 adhere to the following sign conventions: (1) distance along the OAR between two surfaces is positive if measured toward the positive direction of the local Z axis of the first surface; (2) counterclockwise angles are positive; (3) the radius of curvature of a surface is measured from the vertex to the center of curvature and is positive if measured toward the positive direction of the local Z axis; (4) the incident and refractive angles of the OAR, I and I' , at each surface are measured from the surface normal to the OAR; (5) the field and pupil plane tilt angles, θ_b and θ_p , are measured from the field and pupil planes, respectively, to a plane perpendicular to the OAR; and (6) the refractive index is positive when the OAR is traveling toward the positive direction of the local Z axis of the previous surface. Consequently, in Fig. 1, as a way of example, θ_{b1} and $\theta_{b1'}$ are the object and image plane tilt angles for the

Surface 1 and are both positive; t_1 is the distance measured from Surface 1 to Surface 2 along the OAR and is negative; and I'_2 is the refractive angle of OAR after Surface 2 and is negative.

3. PARAXIAL OPTICS IN PLANE-SYMMETRIC SYSTEMS

In paraxial optics, ray heights and angles are approximated to be linearly related; this linear relationship becomes exact as ray heights and angles approach zero. Paraxial optics captures the first-order behavior of rays in optical systems. In the process of deriving the aberration coefficients, the paraxial ray tracing in the sagittal direction was used to define the properties of the ideal image and to approximate the light beam footprint on each optical surface.

A. Paraxial Ray Tracing in the Sagittal Plane

The sagittal direction is the common X axis in all local surface coordinate systems. Sagittal planes are defined as planes containing the X axis and the OAR. Alternatively, tangential planes are perpendicular to the sagittal planes, intersecting along the OAR. It can be derived that the paraxial ray tracing in the sagittal plane follows the following equations:

$$x_{i+1} = x_i + t_i u'_i, \quad (1)$$

$$n'_i u'_i = n_i u_i - \phi_i x_i, \quad (2)$$

$$u_{i+1} = u'_i, \quad (3)$$

where the subscripts, i and $i + 1$, denote the surface number; x is the sagittal ray height on the surface, the sign of which follows the X local coordinate value; u is the tangent of the angle between the sagittal ray and the OAR, the sign of which depends on the sign of x and t ; and ϕ is the oblique optical power defined as

$$\phi_i = \frac{n'_i \cos I'_i - n_i \cos I_i}{R}. \quad (4)$$

An illustration of paraxial ray height and ray angles is shown in Fig. 2. Note that due to the asymmetry between the sagittal and tangential directions, the paraxial ray tracing in the tangential direction is different from that in the sagittal direction.

B. Relation between Object and Image Plane Tilt Angles

By tracing a sagittal marginal ray in paraxial condition, the relation between object and image locations for on-axis conjugates can be derived as the Coddington equation [27], which is shown as

$$\frac{n'_i}{(s'_0)_i} - \frac{n_i}{(s_0)_i} = \phi_i, \quad (5)$$

where s_0 and s'_0 are the object and image distances from the surface i along the OAR, the sign of which is positive if the object or image is on the positive Z axis side of the surface local coordinate system. Using the Coddington equation and Snell's law, it can be derived that for any optical surface i , the object and image plane tilt angles, θ_b and θ'_b , have the relation shown as

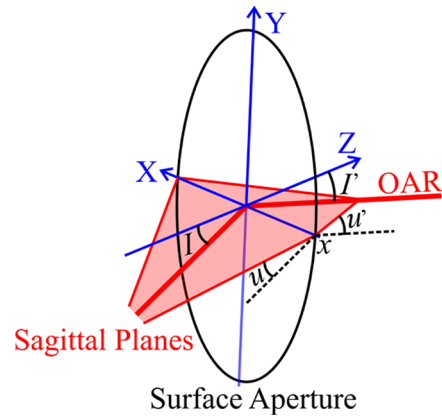


Fig. 2. Illustration of sagittal ray angles and heights.

$$\Delta \left(\frac{1}{\cos I} \left(\frac{\sin I}{R} - \frac{1}{s_0} \tan \theta_b \right) \right)_i = 0, \quad (6)$$

where the operator, $\Delta(\cdot)$, calculates the change of the quantity inside the bracket on refraction. For example, $\Delta(n) = n' - n$, where n and n' are the refractive indices before and after the refraction, respectively.

A similar relationship can be derived for pupil plane tilt angles; a detailed derivation process is included in Supplement 1. Note that when I equals zero as in the rotationally symmetric case, Eq. (6) is reduced to the Scheimpflug condition [28].

4. WAVE ABERRATION FUNCTION EXPANSION FOR PLANE-SYMMETRIC SYSTEMS

In a plane-symmetric system where half of the system is the exact mirror image of the other half, the wavefront aberration function was expanded by Sasian [26] as

$$W(\mathbf{H}, \boldsymbol{\rho}) = \sum_{k,m,n,p,q}^{\infty} W_{2k+n+p, 2m+n+q, n, p, q} (\mathbf{H} \cdot \mathbf{H})^k \times (\boldsymbol{\rho} \cdot \boldsymbol{\rho})^m (\mathbf{H} \cdot \boldsymbol{\rho})^n (\mathbf{i} \cdot \mathbf{H})^p (\mathbf{i} \cdot \boldsymbol{\rho})^q, \quad (7)$$

where W is the wavefront aberration that describes the departure of the real wavefront of a light beam from the reference wavefront; $W_{2k+n+p, 2m+n+q, n, p, q}$ is the aberration coefficient for its associated aberration term; \mathbf{H} is the normalized field vector; and $\boldsymbol{\rho}$ is the normalized pupil vector. \mathbf{H} and $\boldsymbol{\rho}$ lie in the XY plane of the local coordinate systems of the image and exit pupil planes, respectively. The two vectors together define a ray that goes through the system. When the dot products are performed between the field and pupil vectors, the vectors are put into an overlaid coordinate system where all local coordinate systems of surfaces, field, and pupil planes coincide with each other, and \mathbf{i} is the unit vector pointing toward the Y direction of the overlaid coordinate system. An illustration of the overlaid coordinate system is shown in Fig. 1. The terms in the W expansion are grouped by the sum $k + m + n + p + q$. The first four groups are listed in Table 1. In this paper, we expand on Sasian's prior work by presenting the analytical form of the aberration coefficients in the fourth group.

Table 1. First Four Groups of Aberration Terms

First group	W_{00000}		
Second group	$W_{01001}(\mathbf{i} \cdot \boldsymbol{\rho})$ $W_{11100}(\mathbf{H} \cdot \boldsymbol{\rho})$	$W_{10010}(\mathbf{i} \cdot \mathbf{H})$ $W_{20000}(\mathbf{H} \cdot \mathbf{H})$	$W_{02000}(\boldsymbol{\rho} \cdot \boldsymbol{\rho})$
Third group	$W_{02002}(\mathbf{i} \cdot \boldsymbol{\rho})^2$ $W_{03001}(\mathbf{i} \cdot \boldsymbol{\rho})(\boldsymbol{\rho} \cdot \boldsymbol{\rho})$ $W_{21001}(\mathbf{i} \cdot \boldsymbol{\rho})(\mathbf{H} \cdot \mathbf{H})$ $W_{04000}(\boldsymbol{\rho} \cdot \boldsymbol{\rho})^2$ $W_{22000}(\mathbf{H} \cdot \mathbf{H})(\boldsymbol{\rho} \cdot \boldsymbol{\rho})$	$W_{11011}(\mathbf{i} \cdot \boldsymbol{\rho})(\mathbf{i} \cdot \mathbf{H})$ $W_{12101}(\mathbf{i} \cdot \boldsymbol{\rho})(\mathbf{H} \cdot \boldsymbol{\rho})$ $W_{21110}(\mathbf{i} \cdot \mathbf{H})(\mathbf{H} \cdot \boldsymbol{\rho})$ $W_{13100}(\mathbf{H} \cdot \boldsymbol{\rho})(\boldsymbol{\rho} \cdot \boldsymbol{\rho})$ $W_{31100}(\mathbf{H} \cdot \mathbf{H})(\mathbf{H} \cdot \boldsymbol{\rho})$	$W_{20020}(\mathbf{i} \cdot \mathbf{H})^2$ $W_{12010}(\mathbf{i} \cdot \mathbf{H})(\boldsymbol{\rho} \cdot \boldsymbol{\rho})$ $W_{30010}(\mathbf{i} \cdot \mathbf{H})(\mathbf{H} \cdot \mathbf{H})$ $W_{22200}(\mathbf{H} \cdot \boldsymbol{\rho})^2$ $W_{40000}(\mathbf{H} \cdot \mathbf{H})^2$
Fourth group	$W_{03003}(\mathbf{i} \cdot \boldsymbol{\rho})^3$ $W_{30030}(\mathbf{i} \cdot \mathbf{H})^3$ $W_{22002}(\mathbf{i} \cdot \boldsymbol{\rho})^2(\mathbf{H} \cdot \mathbf{H})$ $W_{40020}(\mathbf{i} \cdot \mathbf{H})^2(\mathbf{H} \cdot \mathbf{H})$ $W_{31120}(\mathbf{i} \cdot \mathbf{H})^2(\mathbf{H} \cdot \boldsymbol{\rho})$ $W_{14101}(\mathbf{i} \cdot \boldsymbol{\rho})(\mathbf{H} \cdot \boldsymbol{\rho})(\boldsymbol{\rho} \cdot \boldsymbol{\rho})$ $W_{23201}(\mathbf{i} \cdot \boldsymbol{\rho})(\mathbf{H} \cdot \boldsymbol{\rho})^2$ $W_{32210}(\mathbf{i} \cdot \mathbf{H})(\mathbf{H} \cdot \boldsymbol{\rho})^2$ $W_{50010}(\mathbf{i} \cdot \mathbf{H})(\mathbf{H} \cdot \mathbf{H})^2$ $W_{24000}(\mathbf{H} \cdot \mathbf{H})(\boldsymbol{\rho} \cdot \boldsymbol{\rho})^2$ $W_{33100}(\mathbf{H} \cdot \mathbf{H})(\mathbf{H} \cdot \boldsymbol{\rho})(\boldsymbol{\rho} \cdot \boldsymbol{\rho})$ $W_{51100}(\mathbf{H} \cdot \mathbf{H})^2(\mathbf{H} \cdot \boldsymbol{\rho})$	$W_{12012}(\mathbf{i} \cdot \mathbf{H})(\mathbf{i} \cdot \boldsymbol{\rho})^2$ $W_{04002}(\mathbf{i} \cdot \boldsymbol{\rho})^2(\boldsymbol{\rho} \cdot \boldsymbol{\rho})$ $W_{22020}(\mathbf{i} \cdot \mathbf{H})^2(\boldsymbol{\rho} \cdot \boldsymbol{\rho})$ $W_{13102}(\mathbf{i} \cdot \boldsymbol{\rho})^2(\mathbf{H} \cdot \boldsymbol{\rho})$ $W_{05001}(\mathbf{i} \cdot \boldsymbol{\rho})(\boldsymbol{\rho} \cdot \boldsymbol{\rho})^2$ $W_{23001}(\mathbf{i} \cdot \boldsymbol{\rho})(\mathbf{H} \cdot \mathbf{H})(\boldsymbol{\rho} \cdot \boldsymbol{\rho})$ $W_{32010}(\mathbf{i} \cdot \mathbf{H})(\mathbf{H} \cdot \mathbf{H})(\boldsymbol{\rho} \cdot \boldsymbol{\rho})$ $W_{41110}(\mathbf{i} \cdot \mathbf{H})(\mathbf{H} \cdot \mathbf{H})(\mathbf{H} \cdot \boldsymbol{\rho})$ $W_{06000}(\boldsymbol{\rho} \cdot \boldsymbol{\rho})^3$ $W_{24200}(\mathbf{H} \cdot \boldsymbol{\rho})^2(\boldsymbol{\rho} \cdot \boldsymbol{\rho})$ $W_{42200}(\mathbf{H} \cdot \mathbf{H})(\mathbf{H} \cdot \boldsymbol{\rho})^2$ $W_{60000}(\mathbf{H} \cdot \mathbf{H})^3$	$W_{21021}(\mathbf{i} \cdot \mathbf{H})^2(\mathbf{i} \cdot \boldsymbol{\rho})$ $W_{13011}(\mathbf{i} \cdot \mathbf{H})(\mathbf{i} \cdot \boldsymbol{\rho})(\boldsymbol{\rho} \cdot \boldsymbol{\rho})$ $W_{31011}(\mathbf{i} \cdot \mathbf{H})(\mathbf{i} \cdot \boldsymbol{\rho})(\mathbf{H} \cdot \mathbf{H})$ $W_{22111}(\mathbf{i} \cdot \mathbf{H})(\mathbf{i} \cdot \boldsymbol{\rho})(\mathbf{H} \cdot \boldsymbol{\rho})$ $W_{14010}(\mathbf{i} \cdot \mathbf{H})(\boldsymbol{\rho} \cdot \boldsymbol{\rho})^2$ $W_{23110}(\mathbf{i} \cdot \mathbf{H})(\mathbf{H} \cdot \boldsymbol{\rho})(\boldsymbol{\rho} \cdot \boldsymbol{\rho})$ $W_{32101}(\mathbf{i} \cdot \boldsymbol{\rho})(\mathbf{H} \cdot \mathbf{H})(\mathbf{H} \cdot \boldsymbol{\rho})$ $W_{41001}(\mathbf{i} \cdot \boldsymbol{\rho})(\mathbf{H} \cdot \mathbf{H})^2$ $W_{15100}(\mathbf{H} \cdot \boldsymbol{\rho})(\boldsymbol{\rho} \cdot \boldsymbol{\rho})^2$ $W_{33300}(\mathbf{H} \cdot \boldsymbol{\rho})^3$ $W_{42000}(\mathbf{H} \cdot \mathbf{H})^2(\boldsymbol{\rho} \cdot \boldsymbol{\rho})$

5. PROCESS OF DERIVING THE COEFFICIENTS FOR THE FOURTH GROUP

The derivation of aberration coefficients follows the approach of Hopkins [13]. The optical path difference between a general ray and the OAR is expressed as a Taylor expansion of a function of the field and pupil vectors. The convergence condition of the Taylor expansion is detailed in Supplement 1. The ideal image location and magnification are defined by the paraxial ray trace in the sagittal direction. The case for a single surface with the stop located at the surface and an on-axis object point is derived first as the foundation for the general case with an off-axis object and a stop (aperture stop) away from the surface. With the off-axis object point introduced, the field vector parameter is introduced. For the case where the surface is away from the stop, the ray height at the surface is modeled as a function of the chief and marginal ray heights and the field and pupil vectors. Finally, by grouping and simplifying the terms with the same field and pupil dependence, the analytical formulae of the aberration coefficients for one surface are determined. The total intrinsic aberration coefficients of a system can then be calculated by summing the coefficients for each surface. It should be noted that this does not include induced (extrinsic) aberrations. The detailed derivation process can be found in Supplement 1.

During the derivation, certain assumptions and approximations are made:

- (1) The system is assumed to be plane-symmetric.
- (2) All optical surfaces are assumed to be spherical.
- (3) For a ray defined by a field vector and a pupil vector, the location of the ray intersection at each surface is required to calculate the wave aberration. This ray location is approximated by a linear combination of the paraxial chief ray location and the paraxial marginal ray location shown as

$$\mathbf{r} \approx (\rho_x x_a + x_b) \mathbf{k} + (\rho_y y_a + y_b) \mathbf{i}. \quad (8)$$

In Eq. (8), \mathbf{r} is the location of the ray intersection at the surface, and ρ_x and ρ_y are normalized pupil coordinates ranging from -1 to 1 . The paraxial marginal and chief ray heights at the surface are defined by x_a and x_b in the sagittal direction and y_a and y_b in the tangential direction. \mathbf{k} and \mathbf{i} are the unit vectors in the X and Y directions, respectively. By deriving the paraxial ray height in terms of pupil and field vectors, the marginal and chief ray heights in the sagittal and tangential directions can be shown to have the relationships illustrated in Eqs. (9) and (10),

$$y_a = \frac{\cos \theta_\rho}{\cos I} x_a, \quad (9)$$

$$y_b = \frac{\cos \theta_b}{\cos I} x_b, \quad (10)$$

under the assumption of same field and pupil size in the sagittal and tangential directions, the detailed derivation of which is shown in Supplement 1. This relationship indicates an elliptical beam footprint within paraxial approximation, which is more accurate than the symmetrical approximation where the tangential and sagittal ray heights are assumed equal and is used in deriving all the coefficients presented in Section 6.B. Besides the ellipticity, the beam footprint also experiences higher-order deformation such as a keystone-like deformation discussed by Rogers [29]. Note that the second-order footprint deformation, where ray heights have second-order dependences on pupil and field vectors, has contribution to aberration types in the fourth group. For this paper, we limit the scope to be within the paraxial approximation where the ellipticity of the beam footprint is the main effect.

6. ANALYTICAL FORMULAE FOR THE ABERRATION COEFFICIENTS IN THE FOURTH GROUP

A. Defining Related Mathematical Quantities

To simplify the expressions of the aberration coefficients, we define the following quantities. In Eqs. (11) and (12), we define the quantities A and B as products of the refractive index before a surface, n , and the paraxial incident angle of the sagittal marginal and chief rays, i_a and i_b , respectively. The paraxial angles of the sagittal marginal and chief rays before the surface are denoted by u_a and u_b , respectively:

$$A = ni_a = n \left(u_a + \frac{x_a \cos I}{R} \right), \quad (11)$$

$$B = ni_b = n \left(u_b + \frac{x_b \cos I}{R} \right). \quad (12)$$

We also define the quantity C below, as the product of the index of refraction and the angle before the surface, using the sine of the real incident angle instead of the paraxial angle:

$$C = n \sin I. \quad (13)$$

The Lagrange invariant, Ψ , is defined with paraxial quantities as

$$\Psi = n(u_b x_a - u_a x_b). \quad (14)$$

Factors related to the intrinsic anamorphism between the sagittal and tangential directions are defined as

$$\sigma_1 = \cos(I - \theta_b) - 1, \quad (15)$$

$$\sigma_2 = \frac{\cos \theta_\rho}{\cos I}, \quad (16)$$

$$\sigma_3 = \frac{\cos \theta_b}{\cos I}. \quad (17)$$

B. Aberration Coefficients

In this section, we list the analytical formulae of the aberration coefficients in the fourth group shown in Table 1.

The derivation also includes coefficients from the third group, listed for reference in Eqs. (18)–(32). The coefficients from the fourth group are listed in Eqs. (33)–(67):

$$W_{02002} = -\frac{1}{2} C^2 \Delta \left(\frac{u_a}{n} \right) x_a (2\sigma_2 - 1), \quad (18)$$

$$W_{11011} = \Psi \left[\Delta(\sigma_1) - C \Delta \left(\frac{\sin \theta_b}{n} \right) \right] \sigma_2 - C^2 \Delta \left(\frac{u_a}{n} \right) x_b (\sigma_2 + \sigma_3 - 1), \quad (19)$$

$$W_{20020} = \Psi \left[\Delta(\sigma_1) - C \Delta \left(\frac{\sin \theta_b}{n} \right) \right] \sigma_3 - \frac{1}{2} C^2 \Delta \left(\frac{u_a}{n} \right) \frac{x_b^2}{x_a} (2\sigma_3 - 1), \quad (20)$$

$$W_{03001} = -\frac{1}{2} A C \Delta \left(\frac{u_a}{n} \right) x_a \sigma_2, \quad (21)$$

$$W_{12101} = -B C \Delta \left(\frac{u_a}{n} \right) x_a \sigma_2, \quad (22)$$

$$W_{12010} = -\frac{1}{2} \frac{\Psi C}{R} \Delta \left(\frac{\cos \theta_b}{n} \right) x_a - \frac{1}{2} \Psi \Delta (u_a \sin \theta_b) - \frac{1}{2} A C \Delta \left(\frac{u_a}{n} \right) x_b \sigma_3, \quad (23)$$

$$W_{21001} = -\frac{1}{2} C \Psi \Delta \left(\frac{u_b}{n} \right) \sigma_2 - \frac{1}{2} B C \Delta \left(\frac{u_a}{n} \right) x_b \sigma_2, \quad (24)$$

$$W_{21110} = -\frac{\Psi C}{R} \Delta \left(\frac{\cos \theta_b}{n} \right) x_b - \Psi \Delta (u_b \sin \theta_b) - B C \Delta \left(\frac{u_a}{n} \right) x_b \sigma_3, \quad (25)$$

$$W_{30010} = -\frac{1}{2} C \Psi \Delta \left(\frac{u_b}{n} \right) \frac{x_b}{x_a} \sigma_3 - \frac{1}{2} B C \Delta \left(\frac{u_a}{n} \right) \frac{x_b^2}{x_a} \sigma_3 - \frac{1}{2} \Psi^2 \Delta \left(\frac{\sin \theta_b}{n} \right) \frac{x_b}{x_a^2} - \frac{1}{2} \frac{\Psi C}{R} \Delta \left(\frac{\cos \theta_b}{n} \right) \frac{x_b^2}{x_a} - \frac{1}{2} \Psi \Delta (u_b \sin \theta_b) \frac{x_b}{x_a}, \quad (26)$$

$$W_{04000} = -\frac{1}{8} A^2 \Delta \left(\frac{u_a}{n} \right) x_a, \quad (27)$$

$$W_{13100} = -\frac{1}{2} A B \Delta \left(\frac{u_a}{n} \right) x_a, \quad (28)$$

$$W_{22200} = -\frac{1}{2} B^2 \Delta \left(\frac{u_a}{n} \right) x_a, \quad (29)$$

$$W_{22000} = -\frac{1}{4} A B \Delta \left(\frac{u_a}{n} \right) x_b - \frac{1}{4} A \Psi \Delta \left(\frac{u_b}{n} \right), \quad (30)$$

$$W_{31100} = -\frac{B^2}{2} \Delta \left(\frac{u_a}{n} \right) x_b - \frac{B \Psi}{2} \Delta \left(\frac{u_b}{n} \right), \quad (31)$$

$$W_{40000} = -\frac{1}{8} A (\Psi + B x_a) \Delta \left(\frac{u_a}{n} \right) \frac{x_b^3}{x_a^3} - \frac{1}{4} \Psi (\Psi + B x_a) \Delta \left(\frac{u_b}{n} \right) \frac{x_b}{x_a^2}, \quad (32)$$

$$W_{03003} = \frac{1}{2} C^3 \Delta \left(\frac{u_a^2}{n^2} \right) x_a (3\sigma_2 - 2) - A C \Delta \left(\frac{u_a}{n} \right) x_a (\sigma_2 - 1), \quad (33)$$

$$\begin{aligned}
 W_{12012} = & -\frac{C\Psi}{R} \Delta \left(\frac{\cos \theta_b}{n} \right) x_a (\sigma_2 - 1) - C \Delta \left(\frac{u_a}{n} \right) [Ax_b (\sigma_2 + \sigma_3 - 2) + Bx_a (\sigma_2 - 1)] + \frac{3}{2} C^3 \Delta \left(\frac{u_a^2}{n^2} \right) x_b (2\sigma_2 + \sigma_3 - 2) \\
 & - C\Psi \Delta \left(\frac{\sigma_1 u_a}{n} \right) (2\sigma_2 - 1) - \Psi \Delta (u_a \sin \theta_b) (\sigma_2 - 1) + \frac{3}{2} C^2 \Psi \Delta \left(\frac{u_a \sin \theta_b}{n^2} \right) x_a (2\sigma_2 - 1),
 \end{aligned} \tag{34}$$

$$\begin{aligned}
 W_{21021} = & -\frac{C\Psi}{R} \Delta \left(\frac{\cos \theta_b}{n} \right) x_b (\sigma_2 + \sigma_3 - 2) - C \Delta \left(\frac{u_a}{n} \right) \frac{x_b}{x_a} [Ax_b (\sigma_3 - 1) + Bx_a (\sigma_2 + \sigma_3 - 2)] \\
 & + \frac{3}{2} C^3 \Delta \left(\frac{u_a^2}{n^2} \right) \frac{x_b^2}{x_a} (\sigma_2 + 2\sigma_3 - 2) - 2C\Psi \Delta \left(\frac{\sigma_1 u_a}{n} \right) \frac{x_b}{x_a} (\sigma_2 + \sigma_3 - 1) - \Psi \Delta (u_a \sin \theta_b) \frac{x_b}{x_a} (\sigma_3 - 1) \\
 & - \Psi \Delta (u_b \sin \theta_b) (\sigma_2 - 1) + 3C^2 \Psi \Delta \left(\frac{u_a \sin \theta_b}{n^2} \right) \frac{x_b}{x_a} (\sigma_2 + \sigma_3 - 1) - \Psi^2 \Delta \left(\frac{\sigma_1 \sin \theta_b}{n} \right) \frac{1}{x_a} \sigma_2 + \frac{3}{2} C\Psi^2 \Delta \left(\frac{\sin^2 \theta_b}{n^2} \right) \frac{1}{x_a} \sigma_2,
 \end{aligned} \tag{35}$$

$$\begin{aligned}
 W_{30030} = & -\frac{C\Psi}{R} \Delta \left(\frac{\cos \theta_b}{n} \right) \frac{x_b^2}{x_a} (\sigma_3 - 1) - BC \Delta \left(\frac{u_a}{n} \right) \frac{x_b^2}{x_a} (\sigma_3 - 1) + \frac{1}{2} C^3 \Delta \left(\frac{u_a^2}{n^2} \right) \frac{x_b^3}{x_a^2} (3\sigma_3 - 2) \\
 & - \Psi \Delta (u_b \sin \theta_b) \frac{x_b}{x_a} (\sigma_3 - 1) - C\Psi \Delta \left(\frac{\sigma_1 u_a}{n} \right) \frac{x_b^2}{x_a^2} (2\sigma_3 - 1) \\
 & + \frac{3}{2} C^2 \Psi \Delta \left(\frac{u_a \sin \theta_b}{n^2} \right) \frac{x_b^2}{x_a^2} (2\sigma_3 - 1) - \Psi^2 \Delta \left(\frac{\sigma_1 \sin \theta_b}{n} \right) \frac{x_b}{x_a^2} \sigma_3 + \frac{3}{2} C\Psi^2 \Delta \left(\frac{\sin^2 \theta_b}{n^2} \right) \frac{x_b}{x_a^2} \sigma_3,
 \end{aligned} \tag{36}$$

$$W_{04002} = \frac{3}{4} AC^2 \Delta \left(\frac{u_a^2}{n^2} \right) x_a (2\sigma_2 - 1) - \frac{1}{2} A^2 \Delta \left(\frac{u_a}{n} \right) x_a (\sigma_2 - 1), \tag{37}$$

$$\begin{aligned}
 W_{13011} = & -\frac{1}{2} A \Delta \left(\frac{u_a}{n} \right) x_a [Ax_b (\sigma_3 - 1) + Bx_a (\sigma_2 - 1)] + \frac{3}{2} AC^2 \Delta \left(\frac{u_a^2}{n^2} \right) x_b (\sigma_2 + \sigma_3 - 1) \\
 & - \frac{1}{2} A\Psi \Delta \left(\frac{\sigma_1 u_a}{n} \right) \sigma_2 + \frac{1}{2} \frac{C\Psi}{R} \Delta \left(\frac{u_a \sin(I - \theta_b)}{n} \right) x_a \sigma_2 + \frac{3}{2} AC\Psi \Delta \left(\frac{u_a \sin \theta_b}{n^2} \right) \sigma_2,
 \end{aligned} \tag{38}$$

$$W_{22002} = \frac{3}{4} BC^2 \Delta \left(\frac{u_a^2}{n^2} \right) x_b (2\sigma_2 - 1) + \frac{3}{4} C^2 \Psi \Delta \left(\frac{u_a u_b}{n^2} \right) \frac{x_b}{x_a} (2\sigma_2 - 1) - \frac{1}{2} AB \Delta \left(\frac{u_a}{n} \right) x_b (\sigma_2 - 1) - \frac{1}{2} A\Psi \Delta \left(\frac{u_b}{n} \right) x_b (\sigma_2 - 1), \tag{39}$$

$$\begin{aligned}
 W_{22020} = & -\frac{1}{2} AB \Delta \left(\frac{u_a}{n} \right) x_b (\sigma_3 - 1) - \frac{1}{2} A\Psi \Delta \left(\frac{\sigma_1 u_a}{n} \right) \frac{x_b}{x_a} \sigma_3 + \frac{3}{4} AC^2 \Delta \left(\frac{u_a^2}{n^2} \right) \frac{x_b^2}{x_a} (2\sigma_2 - 1) + \frac{3}{2} AC\Psi \Delta \left(\frac{u_a \sin \theta_b}{n^2} \right) \frac{x_b}{x_a} \sigma_3 \\
 & + \frac{1}{2} \frac{C\Psi}{R} \Delta \left(\frac{u_a \sin(I - \theta_b)}{n} \right) x_b \sigma_3 + \frac{\Psi^2}{4} \left[\frac{2}{R} \Delta \left(\frac{\sin \theta_b \sin(I - \theta_b)}{n} \right) + 3A \Delta \left(\frac{\sin^2 \theta_b}{n^2} \right) \frac{1}{x_a} \right],
 \end{aligned} \tag{40}$$

$$\begin{aligned}
 W_{31011} = & -\frac{1}{2} B \Delta \left(\frac{u_a}{n} \right) \frac{x_b}{x_a} [Ax_b (\sigma_3 - 1) + Bx_a (\sigma_2 - 1)] - \frac{1}{2} \Psi \Delta \left(\frac{u_b}{n} \right) \frac{1}{x_a} [Ax_b (\sigma_3 - 1) + Bx_a (\sigma_2 - 1)] \\
 & + \frac{3}{2} BC^2 \Delta \left(\frac{u_a^2}{n^2} \right) \frac{x_b^2}{x_a} (\sigma_2 + \sigma_3 - 1) + \frac{3}{2} C^2 \Psi \Delta \left(\frac{u_a u_b}{n^2} \right) \frac{x_b}{x_a} (\sigma_2 + \sigma_3 - 1) - \frac{1}{2} B\Psi \Delta \left(\frac{\sigma_1 u_a}{n} \right) \frac{x_b}{x_a} \sigma_2 \\
 & - \frac{1}{2} \Psi^2 \Delta \left(\frac{\sigma_1 u_b}{n} \right) \frac{1}{x_a} \sigma_2 + \frac{1}{2} \frac{C\Psi}{R} \Delta \left(\frac{u_a \sin(I - \theta_b)}{n} \right) \frac{x_b^2}{x_a} \sigma_2 + \frac{3}{2} BC\Psi \Delta \left(\frac{u_a \sin \theta_b}{n^2} \right) \frac{x_b}{x_a} \sigma_2 \\
 & + \frac{3}{2} C\Psi^2 \Delta \left(\frac{u_b \sin \theta_b}{n^2} \right) \frac{1}{x_a} \sigma_2,
 \end{aligned} \tag{41}$$

$$\begin{aligned}
W_{40020} = & -\frac{1}{2}B^2\Delta\left(\frac{u_a}{n}\right)\frac{x_b^2}{x_a}(\sigma_3-1) - \frac{1}{2}B\Psi\Delta\left(\frac{u_b}{n}\right)\frac{x_b}{x_a}(\sigma_3-1) + \frac{3}{4}BC^2\Delta\left(\frac{u_a^2}{n^2}\right)\frac{x_b^3}{x_a^2}(2\sigma_3-1) - \frac{1}{2}B\Psi\Delta\left(\frac{\sigma_1 u_a}{n}\right)\frac{x_b^2}{x_a^2}\sigma_3 \\
& - \frac{1}{2}\Psi^2\Delta\left(\frac{\sigma_1 u_b}{n}\right)\frac{x_b}{x_a^2}\sigma_3 + \frac{3}{4}C^2\Psi\Delta\left(\frac{u_a u_b}{n^2}\right)\frac{x_b^2}{x_a^2}(2\sigma_3-1) + \frac{1}{2}\frac{C\Psi}{R}\Delta\left(\frac{u_a \sin(I-\theta_b)}{n}\right)\frac{x_b^3}{x_a^2}\sigma_3 + \frac{3}{2}BC\Psi\Delta\left(\frac{u_a \sin\theta_b}{n^2}\right)\frac{x_b^2}{x_a^2}\sigma_3 \\
& + \frac{3}{2}C\Psi^2\Delta\left(\frac{u_b \sin\theta_b}{n^2}\right)\frac{x_b}{x_a^2}\sigma_3 + \frac{1}{2}\frac{\Psi^2}{R}\Delta\left(\frac{\sin\theta_b \sin(I-\theta_b)}{n}\right)\frac{x_b^2}{x_a^2} + \frac{3}{4}\Psi^2(\Psi+Bx_a)\Delta\left(\frac{\sin^2\theta_b}{n^2}\right)\frac{x_b}{x_a^3},
\end{aligned} \tag{42}$$

$$W_{13102} = -AB\Delta\left(\frac{u_a}{n}\right)x_a(\sigma_2-1) + \frac{3}{2}BC^2\Delta\left(\frac{u_a^2}{n^2}\right)x_a(2\sigma_2-1), \tag{43}$$

$$\begin{aligned}
W_{22111} = & -B\Delta\left(\frac{u_a}{n}\right)[Ax_b(\sigma_3-1) + Bx_a(\sigma_2-1)] - B\Psi\Delta\left(\frac{\sigma_1 u_a}{n}\right)\sigma_2 + \frac{C\Psi}{R}\Delta\left(\frac{u_a \sin(I-\theta_b)}{n}\right)x_b\sigma_2 \\
& + 3BC^2\Delta\left(\frac{u_a^2}{n^2}\right)x_b(\sigma_2+\sigma_3-1) + 3BC\Psi\Delta\left(\frac{u_a \sin\theta_b}{n^2}\right)\sigma_2,
\end{aligned} \tag{44}$$

$$\begin{aligned}
W_{31120} = & -B^2\Delta\left(\frac{u_a}{n}\right)x_b(\sigma_3-1) + \frac{3}{2}BC^2\Delta\left(\frac{u_a^2}{n^2}\right)\frac{x_b^2}{x_a}(2\sigma_3-1) - B\Psi\Delta\left(\frac{\sigma_1 u_a}{n}\right)\frac{x_b^2}{x_a^2}\sigma_3 + 3BC\Psi\Delta\left(\frac{u_a \sin\theta_b}{n^2}\right)\frac{x_b}{x_a}\sigma_3 \\
& + \frac{C\Psi}{R}\Delta\left(\frac{u_a \sin(I-\theta_b)}{n}\right)\frac{x_b^2}{x_a}\sigma_3 + \frac{\Psi^2}{R}\Delta\left(\frac{\sin\theta_b \sin(I-\theta_b)}{n}\right)\frac{x_b}{x_a} + \frac{3}{2}B\Psi^2\Delta\left(\frac{\sin^2\theta_b}{n^2}\right)\frac{1}{x_a},
\end{aligned} \tag{45}$$

$$W_{05001} = -\frac{1}{8}\frac{AC}{R^2}\Delta\left(\frac{u_a}{n}\right)x_a^3\sigma_2 + \frac{3}{8}A^2C\Delta\left(\frac{u_a^2}{n^2}\right)x_a\sigma_2, \tag{46}$$

$$\begin{aligned}
W_{14010} = & -\frac{1}{8}\frac{C\Psi}{R^3}\Delta\left(\frac{\cos\theta_b}{n}\right)x_a^3 - \frac{1}{8}\frac{AC}{R^2}\Delta\left(\frac{u_a}{n}\right)x_a^2x_b\sigma_3 - \frac{1}{8}\frac{A\Psi}{R}\Delta\left(\frac{u_a \sin(I-\theta_b)}{n}\right)x_a \\
& + \frac{3}{8}A^2C\Delta\left(\frac{u_a^2}{n^2}\right)x_b\sigma_3 + \frac{3}{8}A^2\Psi\Delta\left(\frac{u_a \sin\theta_b}{n^2}\right) - \frac{1}{8}\frac{\Psi}{R^2}\Delta(u_a \sin\theta_b)x_a^2,
\end{aligned} \tag{47}$$

$$W_{14101} = -\frac{1}{2}\frac{AC}{R^2}\Delta\left(\frac{u_a}{n}\right)x_a^2x_b\sigma_2 + \frac{3}{2}ABC\Delta\left(\frac{u_a^2}{n^2}\right)x_a\sigma_2, \tag{48}$$

$$W_{23001} = -\frac{1}{4}\frac{AC}{R^2}\Delta\left(\frac{u_a}{n}\right)x_ax_b^2\sigma_2 + \frac{3}{4}AC\Psi\Delta\left(\frac{u_a u_b}{n^2}\right)\sigma_2 + \frac{3}{4}ABC\Delta\left(\frac{u_a^2}{n^2}\right)x_b\sigma_2, \tag{49}$$

$$\begin{aligned}
W_{23110} = & -\frac{1}{2}\frac{C\Psi}{R^3}\Delta\left(\frac{\cos\theta_b}{n}\right)x_a^2x_b - \frac{1}{2}\frac{AC}{R^2}\Delta\left(\frac{u_a}{n}\right)x_ax_b^2\sigma_3 + \frac{1}{2}\frac{\Psi}{R}(Ax_b + Bx_a)\Delta\left(\frac{u_a \sin(I-\theta_b)}{n}\right) \\
& + \frac{1}{2}ABC\Delta\left(\frac{u_a^2}{n^2}\right)x_b\sigma_3 - \frac{1}{2}\frac{\Psi}{R^2}\Delta(u_a \sin\theta_b)x_ax_b + \frac{3}{2}AB\Psi\Delta\left(\frac{u_a \sin\theta_b}{n^2}\right),
\end{aligned} \tag{50}$$

$$W_{23201} = -\frac{1}{2}\frac{AC}{R^2}\Delta\left(\frac{u_a}{n}\right)x_ax_b^2\sigma_2 + \frac{3}{2}B^2C\Delta\left(\frac{u_a^2}{n^2}\right)x_a\sigma_2, \tag{51}$$

$$\begin{aligned}
W_{32010} = & -\frac{1}{4}\frac{C\Psi}{R^3}\Delta\left(\frac{\cos\theta_b}{n}\right)x_ax_b^2 - \frac{1}{4}\frac{AC}{R^2}\Delta\left(\frac{u_a}{n}\right)x_b^3\sigma_3 + \frac{3}{4}ABC\Delta\left(\frac{u_a^2}{n^2}\right)\frac{x_b^2}{x_a}\sigma_3 + \frac{3}{4}AC\Psi\Delta\left(\frac{u_a u_b}{n^2}\right)\sigma_3 \\
& + \frac{1}{2}\frac{B\Psi}{R}\Delta\left(\frac{\sin(I-\theta_b)}{n}\right)x_b + \frac{1}{4}\frac{\Psi^3}{R}\Delta\left(\frac{\sin(I-\theta_b)}{n^2}\right)\frac{1}{x_a} - \frac{1}{4}\frac{\Psi}{R^2}\Delta(u_a \sin\theta_b)x_b^2 + \frac{3}{4}AB\Psi\Delta\left(\frac{u_a \sin\theta_b}{n^2}\right) \\
& + \frac{3}{4}A\Psi^2\Delta\left(\frac{u_b \sin\theta_b}{n^2}\right)\frac{1}{x_a},
\end{aligned} \tag{52}$$

$$W_{32101} = -\frac{1}{2} \frac{AC}{R^2} \Delta \left(\frac{u_a}{n} \right) x_b^3 \sigma_2 + \frac{3}{2} B^2 C \Delta \left(\frac{u_a^2}{n^2} \right) x_b \sigma_2 + \frac{3}{2} BC \Psi \Delta \left(\frac{u_a u_b}{n^2} \right) \sigma_2, \tag{53}$$

$$W_{32210} = -\frac{1}{2} \frac{C\Psi}{R^3} \Delta \left(\frac{\cos \theta_b}{n} \right) x_a x_b^2 - \frac{1}{2} \frac{AC}{R^2} \Delta \left(\frac{u_a}{n} \right) x_b^2 \sigma_3 + \frac{3}{2} B^2 C \Delta \left(\frac{u_a^2}{n^2} \right) x_b \sigma_3 \\ + \frac{B\Psi}{R} \Delta \left(\frac{u_a \sin(I - \theta_b)}{n} \right) x_b - \frac{1}{2} \frac{\Psi}{R^2} \Delta (u_a \sin \theta_b) x_b^2 + \frac{3}{2} B\Psi \Delta \left(\frac{u_a \sin \theta_b}{n^2} \right), \tag{54}$$

$$W_{41110} = -\frac{1}{2} \frac{C\Psi}{R^3} \Delta \left(\frac{\cos \theta_b}{n} \right) x_b^3 - \frac{1}{2} \frac{AC}{R^2} \Delta \left(\frac{u_a}{n} \right) \frac{x_b^4}{x_a} \sigma_3 + \frac{3}{2} B^2 C \Delta \left(\frac{u_a^2}{n^2} \right) \frac{x_b^2}{x_a} \sigma_3 \\ + \frac{3}{2} BC \Delta \left(\frac{u_a u_b}{n^2} \right) \frac{x_b}{x_a} \sigma_3 + \frac{B\Psi}{R} \Delta \left(\frac{u_a \sin(I - \theta_b)}{n} \right) \frac{x_b^2}{x_a} + \frac{1}{2} \frac{\Psi^2}{R} \Delta \left(\frac{u_b \sin(I - \theta_b)}{n^2} \right) \frac{x_b}{x_a} \\ - \frac{1}{2} \frac{\Psi}{R^2} \Delta (u_a \sin \theta_b) \frac{x_b^3}{x_a} + \frac{3}{2} B^2 \Psi \Delta \left(\frac{u_a \sin \theta_b}{n^2} \right) \frac{x_b}{x_a} + \frac{3}{2} B\Psi^2 \Delta \left(\frac{u_b \sin \theta_b}{n^2} \right) \frac{1}{x_a}, \tag{55}$$

$$W_{41001} = -\frac{1}{8} \frac{AC}{R^2} \Delta \left(\frac{u_a}{n} \right) \frac{x_b^4}{x_a} \sigma_2 + \frac{3}{8} B^2 C \Delta \left(\frac{u_a^2}{n^2} \right) \frac{x_b^2}{x_a} \sigma_2 + \frac{3}{4} BC \Psi \Delta \left(\frac{u_a u_b}{n^2} \right) \frac{x_b}{x_a} \sigma_2 + \frac{3}{8} C\Psi^2 \Delta \left(\frac{u_b^2}{n^2} \right) \frac{1}{x_a} \sigma_2, \tag{56}$$

$$W_{50010} = -\frac{1}{8} \frac{C\Psi}{R^3} \Delta \left(\frac{\cos \theta_b}{n} \right) \frac{x_b^4}{x_a} - \frac{1}{8} \frac{AC}{R^2} \Delta \left(\frac{u_a}{n} \right) \frac{x_b^5}{x_a^2} \sigma_3 + \frac{3}{8} B^2 C \Delta \left(\frac{u_a^2}{n^2} \right) \frac{x_b^3}{x_a^2} \sigma_3 + \frac{3}{4} BC \Psi \Delta \left(\frac{u_a u_b}{n^2} \right) \frac{x_b^2}{x_a^2} \sigma_3 \\ + \frac{3}{8} C\Psi^2 \Delta \left(\frac{u_b^2}{n^2} \right) \frac{x_b}{x_a^2} \sigma_3 + \frac{1}{4} \frac{B\Psi}{R} \Delta \left(\frac{u_a \sin(I - \theta_b)}{n} \right) \frac{x_b^3}{x_a^2} + \frac{1}{4} \frac{\Psi^2}{R} \Delta \left(\frac{u_b \sin(I - \theta_b)}{n^2} \right) \frac{x_b^2}{x_a^2} \\ - \frac{1}{8} \frac{\Psi}{R^2} \Delta (u_a \sin \theta_b) \frac{x_b^4}{x_a^2} + \frac{3}{8} A\Psi(\Psi + Bx_a) \Delta \left(\frac{u_a \sin \theta_b}{n^2} \right) \frac{x_b^3}{x_a^4} + \frac{3}{4} \Psi^2(\Psi + Bx_a) \Delta \left(\frac{u_b \sin \theta_b}{n^2} \right) \frac{x_b}{x_a^3}, \tag{57}$$

$$W_{06000} = -\frac{1}{16} \frac{A^2}{R^2} \Delta \left(\frac{u_a}{n} \right) x_a^3 + \frac{1}{16} A^3 \Delta \left(\frac{u_a^2}{n^2} \right) x_a, \tag{58}$$

$$W_{15100} = -\frac{1}{8} \frac{A}{R^2} (2Ax_b + Bx_a) \Delta \left(\frac{u_a}{n} \right) x_a^2 + \frac{3}{8} A^2 B \Delta \left(\frac{u_a^2}{n^2} \right) x_a, \tag{59}$$

$$W_{24000} = -\frac{1}{16} \frac{A}{R^2} (2Ax_b + Bx_a) \Delta \left(\frac{u_a}{n} \right) x_a x_b - \frac{1}{16} \frac{A\Psi}{R^2} \Delta \left(\frac{u_a}{n} \right) x_a^2 + \frac{3}{16} A^2 B \Delta \left(\frac{u_a^2}{n^2} \right) x_b + \frac{3}{16} A^2 \Psi \Delta \left(\frac{u_a u_b}{n^2} \right), \tag{60}$$

$$W_{24200} = -\frac{1}{4} \frac{A}{R^2} (Ax_b + 2Bx_a) \Delta \left(\frac{u_a}{n} \right) x_a x_b + \frac{3}{4} AB \Delta \left(\frac{u_a^2}{n^2} \right) x_a, \tag{61}$$

$$W_{33300} = -\frac{1}{2} \frac{AB}{R^2} \Delta \left(\frac{u_a}{n} \right) x_a x_b^2 + \frac{1}{2} B^2 \Delta \left(\frac{u_a^2}{n^2} \right) x_a, \tag{62}$$

$$W_{33100} = -\frac{1}{4} \frac{A}{R^2} (Ax_b + 2Bx_a) \Delta \left(\frac{u_a}{n} \right) x_b^2 - \frac{1}{4} \frac{A\Psi}{R^2} \Delta \left(\frac{u_b}{n} \right) x_a x_b + \frac{3}{4} AB \Psi \Delta \left(\frac{u_a u_b}{n^2} \right) + \frac{3}{4} AB^2 \Delta \left(\frac{u_a^2}{n^2} \right) x_b, \tag{63}$$

$$W_{42200} = -\frac{3}{4} \frac{AB}{R^2} \Delta \left(\frac{u_a}{n} \right) x_b^3 - \frac{1}{4} \frac{A\Psi}{R^2} \Delta \left(\frac{u_b}{n} \right) x_b^2 + \frac{3}{4} B^3 \Delta \left(\frac{u_a^2}{n^2} \right) x_b + \frac{3}{4} B^2 \Psi \Delta \left(\frac{u_a u_b}{n^2} \right), \tag{64}$$

$$W_{42000} = -\frac{1}{16} \frac{A}{R^2} (Ax_b + 2Bx_a) \Delta \left(\frac{u_a}{n} \right) \frac{x_b^3}{x_a} - \frac{1}{8} \frac{A\Psi}{R^2} \Delta \left(\frac{u_b}{n} \right) x_b^2 + \frac{3}{16} AB^2 \Delta \left(\frac{u_a^2}{n^2} \right) \frac{x_b^2}{x_a} \\ + \frac{3}{8} AB \Psi \Delta \left(\frac{u_a u_b}{n^2} \right) \frac{x_b}{x_a} + \frac{3}{16} A\Psi^2 \Delta \left(\frac{u_b^2}{n^2} \right) \frac{1}{x_a}, \tag{65}$$

$$\begin{aligned}
W_{51100} = & -\frac{3}{8} \frac{AB}{R^2} \Delta \left(\frac{u_a}{n} \right) \frac{x_b^4}{x_a} - \frac{1}{4} \frac{A\Psi}{R^2} \Delta \left(\frac{u_b}{n} \right) \frac{x_b^3}{x_a} \\
& + \frac{3}{8} B^3 \Delta \left(\frac{u_a^2}{n^2} \right) \frac{x_b^2}{x_a} + \frac{3}{4} B^2 \Psi \Delta \left(\frac{u_a u_b}{n^2} \right) \frac{x_b}{x_a} \\
& + \frac{3}{8} B \Psi^2 \Delta \left(\frac{u_b^2}{n^2} \right) \frac{1}{x_a}, \tag{66}
\end{aligned}$$

$$\begin{aligned}
W_{60000} = & -\frac{1}{16} \frac{AB}{R^2} \Delta \left(\frac{u_a}{n} \right) \frac{x_b^5}{x_a^2} - \frac{1}{16} \frac{A\Psi}{R^2} \Delta \left(\frac{u_b}{n} \right) \frac{x_b^4}{x_a^2} \\
& + \frac{1}{16} (\Psi^3 + B^3 x_a^3) \Delta \left(\frac{u_a^2}{n^2} \right) \frac{x_b^3}{x_a^3} \\
& + \frac{3}{16} A\Psi (\Psi + B x_a) \Delta \left(\frac{u_a u_b}{n^2} \right) \frac{x_b^3}{x_a^4} \\
& + \frac{3}{16} \Psi^2 (\Psi + B x_a) \Delta \left(\frac{u_b^2}{n^2} \right) \frac{x_b}{x_a^3}. \tag{67}
\end{aligned}$$

7. EXAMPLE

A one-surface system is used as an example to compare the aberration coefficients derived from the theory and computed from ray tracing with CODE V. As shown in Fig. 3, a collimated beam with a 50-mm diameter is incident on a tilted concave mirror and is focused on the paraxial image plane. The mirror serves as the stop and has a tilted angle $I = -20^\circ$ and a radius of curvature $R = -100$ mm. The distance of the paraxial image plane can be calculated using Eqs. (1)–(4) to be $d = -53.2$ mm. Therefore, the system is approximately F/1.

To compute the wavefront error, optical paths of real rays are calculated from a starting plane perpendicular to the incident

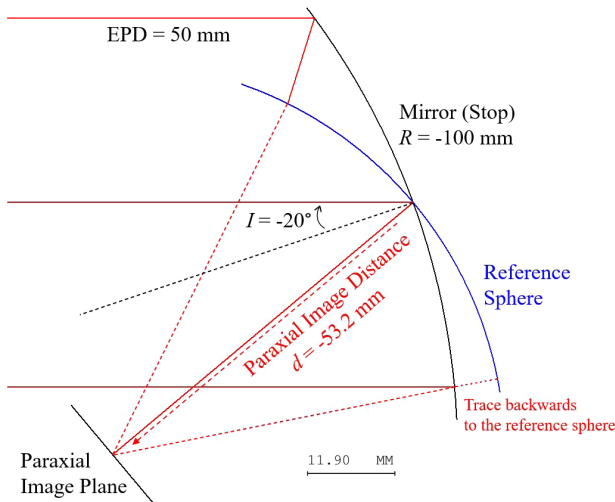


Fig. 3. One-surface system with a concave mirror (tilted angle $I = -20^\circ$, radius of curvature $R = -100$ mm). A 50-mm diameter beam is incident on the mirror and focused onto the paraxial image plane located $d = -53.2$ mm from the mirror after the reflection. In blue, a reference sphere located at the exit pupil to which the optical path is calculated. Solid red lines are real rays, and the dashed red lines are approximate ray paths for illustration, not real rays.

beam to a reference sphere located at the exit pupil which is at the same location as the mirror as shown in blue in Fig. 3. The reference sphere is centered at the paraxial image point. The location of the starting plane can be chosen arbitrarily in object space. The wavefront error of a ray is calculated by subtracting the optical path of the ray from that of the chief ray, producing a map of wavefront error of rays in different pupil locations. Note that some rays need to be traced backwards after the reflection to reach the reference sphere. The optical path of the backwards tracing is signed negative. In other cases, the optical path is always positive regardless of the sign of the refractive index.

To find the aberration coefficients computationally, a Fringe Zernike polynomial [30] is fitted to the wavefront error map, leveraging the orthogonality of the polynomial for more accurate fitting. In this case, the map is sampled at 201 points over the pupil diameter, and a 37-term Fringe Zernike polynomial is fitted to the data. From the definition of the Fringe Zernike terms, wavefront aberration coefficients can be approximated as

$$\begin{aligned}
W_{02000} \approx & 2Z_4 + Z_5 - 6Z_9 - 3Z_{12} + 12Z_{16} \\
& + 6Z_{21} - 20Z_{25} - 10Z_{32} + 30Z_{36} - 42Z_{37}, \tag{68}
\end{aligned}$$

$$W_{02002} \approx -2Z_5 + 6Z_{12} - 12Z_{21} + 20Z_{32}, \tag{69}$$

$$\begin{aligned}
W_{03001} \approx & 3Z_8 + 3Z_{11} - 12Z_{15} - 12Z_{20} + 30Z_{24} \\
& + 30Z_{31} - 60Z_{35}, \tag{70}
\end{aligned}$$

$$\begin{aligned}
W_{04000} \approx & -6Z_9 + 4Z_{12} - 30Z_{16} - Z_{17} - 20Z_{21} \\
& + 90Z_{25} - 5Z_{28} + 60Z_{32} - 210Z_{36} + 420Z_{37}, \tag{71}
\end{aligned}$$

$$W_{03003} \approx -4Z_{11} + 16Z_{20} - 20Z_{27} - 40Z_{31}, \tag{72}$$

$$W_{04002} \approx -8Z_{12} - 8Z_{17} + 40Z_{21} + 40Z_{28} - 120Z_{32}, \tag{73}$$

$$W_{05001} \approx 10Z_{15} + 15Z_{20} - 60Z_{24} + 5Z_{27} - 90Z_{31} + 210Z_{35}, \tag{74}$$

$$\begin{aligned}
W_{06000} \approx & 20Z_{16} + 15Z_{21} - 140Z_{25} + 6Z_{28} \\
& - 105Z_{32} + 560Z_{36} - 1680Z_{36}. \tag{75}
\end{aligned}$$

Table 2 lists the coefficients calculated from the theoretical formulae and from ray tracing and fitting. In this example, only the coefficients with no field dependence are calculated. Note that the theoretical value of W_{02000} is zero due to the nature of the paraxial image plane. The results from both methods are in general agreement. The differences between the results can come from several possible sources including the approximation used during the derivation of the analytical formulae, omitted contributions from higher-order Fringe Zernike terms, and numerical error resulting from sampling and fitting. The results also show that besides the main aberration contributions from the constant astigmatism, W_{02002} , and constant coma, W_{03001} ,

Table 2. Aberration Coefficients Calculated from the Theoretical Formulae and from Ray Tracing and Fitting for the System Shown in Fig. 3

Wavelength: 587.6 nm	From the Theoretical Formulae (Waves)	From Ray Tracing and Fitting (Waves)
W_{02000}	0	-1.691
W_{02002}	1319	1324
W_{03001}	854.7	968.3
W_{04000}	137.8	180.7
W_{03003}	-121.0	-124.7
W_{04002}	-182.9	-142.1
W_{05001}	-57.35	-53.27
W_{06000}	-3.233	-7.318

the aberration types from the fourth group, W_{03003} , W_{04002} , and W_{05001} , also have non-negligible contributions.

8. CONCLUSION

The fourth-group's aberration coefficients for plane-symmetric optical systems are derived as functions of the first-order system parameters and the paraxial chief and marginal ray angles and heights. The aberration coefficients are useful for providing valuable information on the amount, types, and surface balancing of imaging aberration in an optical system, as well as how the aberration is affected by first-order system parameters and the paraxial sagittal chief and marginal ray angles and heights. The coefficients expand the aberration theory for plane-symmetric systems and enable the analytical calculation of their higher-order aberrations. Access to these computations is timely because systems that demand more and more stringent specifications, such as faster F -numbers and larger fields of view, are undoubtedly emerging.

Funding. National Science Foundation I/UCRC Center for Freeform Optics (IIP-1338877, IIP-1338898, IIP-1822026, IIP-1822049); National Aeronautics and Space Administration (NASA) (80NSSC21K1838).

Acknowledgment. We thank Aaron Bauer for simulating discussion for this work.

Disclosures. The authors declare no conflicts of interests.

Data availability. Data underlying the results presented in this paper are not publicly available at this time but may be obtained from the authors upon reasonable request.

Supplemental document. See Supplement 1 for supporting content.

REFERENCES AND NOTES

- J. P. Rolland, M. A. Davies, T. J. Suleski, C. Evans, A. Bauer, J. C. Lambropoulos, and K. Falaggis, "Freeform optics for imaging," *Optica* **8**, 161–176 (2021).
- A. Offner, "Unit power imaging catoptric anastigmat," U.S. patent 3,748,015 (July 24, 1973).
- L. Cook, "Three mirror anastigmatic optical system," U.S. patent 4,265,510 (May 5, 1981).
- A. E. Conrady, "Decentered lens-systems," *Mon. Not. R. Astron. Soc.* **79**, 384–390 (1919).
- L. I. Epstein, "The aberrations of slightly decentered optical systems," *J. Opt. Soc. Am.* **39**, 847–853 (1949).
- L. Cook, "Three-mirror anastigmat used off-axis in aperture and field," *Proc. SPIE* **0183**, 207–211 (1979).
- C. Wynne, "The primary aberrations of anamorphic lens systems," *Proc. Phys. Soc. B* **67**, 529 (1954).
- P. Sands, "Aberration coefficients of double-plane-symmetric systems," *J. Opt. Soc. Am.* **63**, 425–430 (1973).
- R. A. Buchroeder, "Tilted component optical systems," Ph.D. dissertation (The University of Arizona, 1976).
- A. Bauer and J. P. Rolland, "Design of a freeform electronic viewfinder coupled to aberration fields of freeform optics," *Opt. Express* **23**, 28141–28153 (2015).
- A. Bauer, M. Pesch, J. Muschaweck, F. Leupelt, and J. P. Rolland, "All-reflective electronic viewfinder enabled by freeform optics," *Opt. Express* **27**, 30597–30605 (2019).
- A. Bauer and J. P. Rolland, "Roadmap for the unobscured three-mirror freeform design space," *Opt. Express* **29**, 26736–26744 (2021).
- H. H. Hopkins, *Wave Theory of Aberrations* (Clarendon, 1950).
- R. Shack and K. Thompson, "Influence of alignment errors of a telescope system on its aberration field," *Proc. SPIE* **251**, 146–153 (1980).
- K. Thompson, "Description of the third-order optical aberrations of near-circular pupil optical systems without symmetry," *J. Opt. Soc. Am. A* **22**, 1389–1401 (2005).
- K. P. Thompson, "Multinodal fifth-order optical aberrations of optical systems without rotational symmetry: spherical aberration," *J. Opt. Soc. Am. A* **26**, 1090–1100 (2009).
- K. P. Thompson, "Multinodal fifth-order optical aberrations of optical systems without rotational symmetry: the comatic aberrations," *J. Opt. Soc. Am. A* **27**, 1490–1504 (2010).
- K. P. Thompson, "Multinodal fifth-order optical aberrations of optical systems without rotational symmetry: the astigmatic aberrations," *J. Opt. Soc. Am. A* **28**, 821–836 (2011).
- K. Fuerschbach, J. P. Rolland, and K. P. Thompson, "Theory of aberration fields for general optical systems with freeform surfaces," *Opt. Express* **22**, 26585–26606 (2014).
- A. Bauer, E. M. Schiesser, and J. P. Rolland, "Starting geometry creation and design method for freeform optics," *Nat. Commun.* **9**, 1756 (2018).
- Z. Tang and H. Gross, "Extended aberration analysis in symmetry-free optical systems - part I: method of calculation," *Opt. Express* **29**, 39967–39982 (2021).
- Z. Tang and H. Gross, "Extended aberration analysis in symmetry-free optical systems - part II: evaluation and application," *Opt. Express* **29**, 42020–42036 (2021).
- J. Caron and S. Bäumer, "Aberrations of plane-symmetrical mirror systems with freeform surfaces. Part I: generalized ray-tracing equations," *J. Opt. Soc. Am. A* **38**, 80–89 (2021).
- J. Caron and S. Bäumer, "Aberrations of plane-symmetrical mirror systems with freeform surfaces. Part II: closed-form aberration formulas," *J. Opt. Soc. Am. A* **38**, 90–98 (2021).
- J. Caron, T. Ceccotti, and S. Bäumer, "Progress in aberration theory for freeform off-axis mirror systems," *Proc. SPIE* **12078**, 120780G (2021).
- J. M. Sasian, "How to approach the design of a bilateral symmetric optical system," *Opt. Eng.* **33**, 2045–2061 (1994).
- H. Coddington, *A Treatise on the Reflexion and Refraction of Light being Part 1 of A System of Optics* (Cambridge University, 1829).
- T. Scheimpflug, "Improved method and apparatus for the systematic alteration or distortion of plane pictures and images by means of lenses and mirrors for photography and for other purposes," British patent No. 1196 (May 12, 1904).
- J. Rogers, "A comparison of anamorphic, keystone, and Zernike surface types for aberration correction," *Proc. SPIE* **7652**, 129–136 (2010).
- The Fringe Zernike polynomial was developed by John Loomis at the University of Arizona, Optical Sciences Center in the 1970s, and is described on page 712 of the CODE V® Version 11.5 Lens System Setup Reference Manual (Synopsys, Inc., 2021).